Elaboration by spray pyrolysis and characterization in the VUV range of phosphor particles with spherical shape and micronic size

Nicolas Joffin, Bruno Caillier, Jeannette Dexpert-Ghys, Marc Verelst, Guy Baret, Alain Garcia, Philippe Guillot, Jacques Galy, Robert Mauricot, Sylvie Schamm-Chardon

Elaboration by spray pyrolysis and characterization in the VUV range of phosphor particles with spherical shape and micronic size

Nicolas Joffin[1,2], Bruno Caillier[3], Jeannette Dexpert-Ghys[1], Marc Verelst[1], Guy Baret[2], Alain Garcia[4], Philippe Guillot[3], Jacques Galy[3], Robert Mauricot[1] and Sylvie Schamm[1]

[1] CEMES-CNRS, 29 rue Jeanne Marvig 31055 Toulouse, France
[2] DGTec SAS, 178 rue de Mayoussard F-38430 Moirans, France

[3] CPAT, Université Paul Sabatier, 118 route de Narbonne, Bat3R2, 31062 Toulouse, France
[4] ICMCB-CNRS, 87 Avenue du Docteur Schweitzer 33608 Pessac, France

E-mail: jdexpert@cemes.fr and info@dgtec.fr

Abstract
Y_2O_3 : Eu and Zn_2SiO_4 : Mn are the red and green phosphors actually used in plasma display panels. These phosphors have been prepared by spray pyrolysis synthesis and thermal post-treatments. Their optical properties in the vacuum ultraviolet (VUV) energy range have been investigated. The absorption coefficients have been extracted from electron energy loss spectroscopy. The luminescence properties of phosphors from spray pyrolysis have been characterized under UV or VUV excitations with different dedicated experimental set-ups: excitation spectroscopy, measurements of luminescence efficiencies under Hg lamp, pure Xe and Ne–Xe discharges, determinations of luminescence decay times under plasma excitation. The characteristics have been compared with those of corresponding commercial phosphors.

1. Introduction

Spray pyrolysis is a promising way of synthesizing spherical shaped and micronic sized particles in a very large range of compositions and applications [1]. We have used this technique to prepare red and green phosphors ($Y_2O_3 : Eu^{3+}$ and $Zn_2SiO_4 : Mn^{2+}$, respectively) for plasma display panels (PDPs). In this paper, the different methods employed for investigation of the optical properties in the vacuum ultraviolet (VUV) energy range of the prepared powders are described. The intrinsic absorption of the phosphors has been measured by electron energy loss spectroscopy (EELS) in a transmission electron microscope (TEM). The luminescence excitation spectra of the samples have been recorded in the proper spectral range and the photoluminescence efficiencies under plasma excitation measured with two different set-ups. The luminescence decays have been analysed and the decay times (measured at $I_0/10$) determined. The characteristics of the red and green phosphors from spray pyrolysis (SPR and SPG) have been compared with those of the corresponding commercial phosphors (CPR and CPG). It is one of the objectives of this work to consider in detail the various experimental set-ups, in order to perform a critical analysis of the results.

2. Experimental

2.1. Samples synthesis and structural characterizations

Powder samples were prepared using a laboratory scale spray pyrolysis process that we have described previously [2, 3]. The piezoelectric pellet frequency was 2.4 MHz, the air flow was maintained constant at 5 litre min^{-1}, and the drying area was about 100°C. For the SPR samples, only the composition $Y_{1.93}Eu_{0.07}O_3$ (that of the CPR, purchased from Kyokko)

has been synthesized. A solution of yttrium and europium nitrates in appropriate proportions was decomposed at 700°C. The powder was further annealed under air at temperatures from 900°C to 1400°C, in order to complete the crystallization of the cubic oxide. Samples with different post-synthesis thermal treatments are denoted hereafter SPR1–3. The resulting powders are made of hollow spheres: an empty core and a polycrystalline shell less than 100 nm thick, as described previously in more detail [4, 5]. TEM and scanning electron microscopy (SEM) images of SPR3 are shown in figure 1. The variation of the average crystal size has been monitored by x-ray diffraction. The inter-particle agglomeration has been estimated by considering the mean equivalent diameter from the volume of the spheres, D_v50, measured with a Malvern Mastersizer S laser size analyser. The samples SPR1–3 are characterized by the same $D_v50 = 2.2\,\mu$m and by an increasing average crystal size with heat treatment (table 1).

For the SPG1–4 phosphors $Zn_{2-2x}Mn_{2x}SiO_4$, samples with $x = 0.02$–0.05 have been prepared starting from a mixture of zinc and manganese nitrates and of a colloidal silica solution in relevant proportions. The decomposition was performed at 500°C. The spherical particles at this stage are made of crystallized ZnO and amorphous silica. An additional thermal treatment is then applied in order to complete the formation of the luminescent manganese-doped willemite phase, checked by x-ray diffraction. Simultaneously there is an increase in the crystal size. Unlike what has been observed for $Y_2O_3:Eu^{3+}$, the annealing of $Zn_2SiO_4:Mn^{2+}$ samples induces different variations of D_v50 with temperature when the Mn content is varied [2]. In this study, the SPG1–4 samples have been all submitted to the same thermal treatment at 1300°C for 1 h, and the D_v50 values are gathered in table 2. The morphology of the green phosphors, imaged by TEM or by SEM (figure 2), is different from that of the red phosphor. There is an important open porosity (macroporosity), homogeneously distributed in the spheres, but no core–shell contrast is observed. The CPG was purchased from Nishia, and its formula is $Zn_{1.92}Mn_{0.08}SiO_4$ ($x = 0.04$).

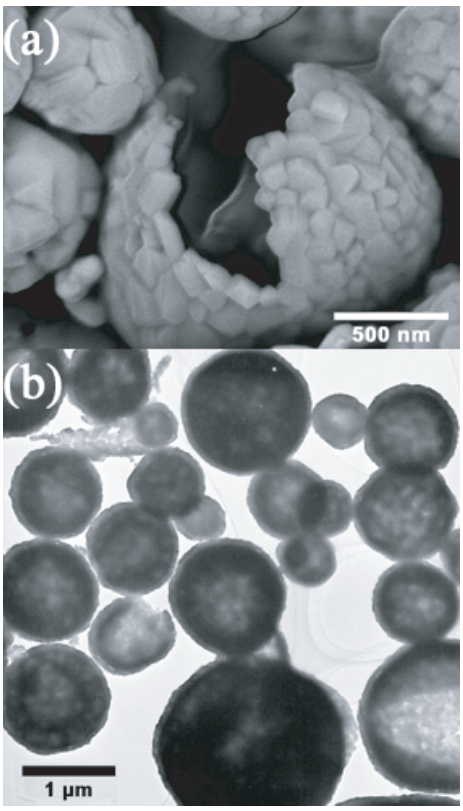

Figure 1. (*a*) SEM and (*b*) TEM imaging of SPR3 powder.

2.2. Absorption coefficient measurement by EELS

Quantitative information on optical constants such as the absorption coefficient can be extracted with a good spatial resolution, down to the nanometric range, by performing EELS experiments in a TEM. This information is obtained from exploitation of the low energy-loss domain of the EELS spectrum, which extends over a large spectral domain covering the visible–UV–soft x-rays range.

The measurements were performed on a Philips CM20 TEM operating at 100 kV. The microscope is equipped with a Gatan PEELS spectrometer, the energy resolution (FWHM of the zero-loss peak) and dispersion of which were 0.6 eV and 0.1 eV per channel, respectively. Spectra were acquired in the image mode, and the diameter of the analysed area was a few tens of nanometres. The spectra are corrected for noise and detector gain via the Gatan procedure. The samples analysed were SPR2 and SPG4 (table 3). Undoped willemite, Zn_2SiO_4, from spray pyrolysis was investigated, as well as pure cubic C–Y_2O_3 purchased from Rhodia. The low-loss spectra were processed using home-made software [6, 7]. It consists of different stages [8], pertaining to the extraction of the low-loss function $\mathrm{Im}(-1/\varepsilon(E))$ from an experimental spectrum $I(E)$, after which $\mathrm{Re}(-1/\varepsilon(E))$ is obtained from the Kramers–Krönig relation, thereby yielding the real part, $\varepsilon_1(E)$, and the imaginary part, $\varepsilon_2(E)$, of the dielectric function. The absolute scale of $\mathrm{Im}(-1/\varepsilon(E))$ is obtained by use of the Kramers–Krönig sum rule at zero energy. $\varepsilon(0)$ is taken to be the square of the refractive index. The variation of some optical constants with energy or wavelength can then be deduced, such as the refractive index, n, the extinction coefficient, κ, the absorption coefficient, α and the reflectance, R. In this paper, we concentrate on the absorption coefficient.

Table 1. Structural characteristics, luminescence efficiencies and decay times of the red phosphors.

Sample	Crystal size (nm)	Particle diameter, D_v50 (μm)	254 nm Hg lamp	254 nm spectroscopy	147 nm spectroscopy	Plasma CPAT set-up	Plasma DGTec set-up	τ_{10} (ms)
CPR	95	3.5	100	100	100	100	100	5
SPR1	42	2.2	56	56	63	44	53	3.7
SPR2	53	2.2	59	59	74	62	85	3.7
SPR3	85	2.2	58	58	80	91	105	4.3

Table 2. Structural characteristics, luminescence efficiencies and decay times of the green phosphors.

Sample	Mn/(Mn + Zn) (%)	Particle diameter, D_v50 (μm)	254 nm Hg lamp	254 nm spectroscopy	147 nm spectroscopy	Plasma CPAT set-up	Plasma DGTec set-up	τ_{10} (ms)
CPG	4	8	100	100	100	100	100	17.5
SPG1	2	7.8	72	73	100	124	132	36
SPG2	3	5.2	72	75	100	116	87	29
SPG3	4	4.8	74	71	75	88	71	17.5
SPG4	5	4.4	66	70	75	48	49	12

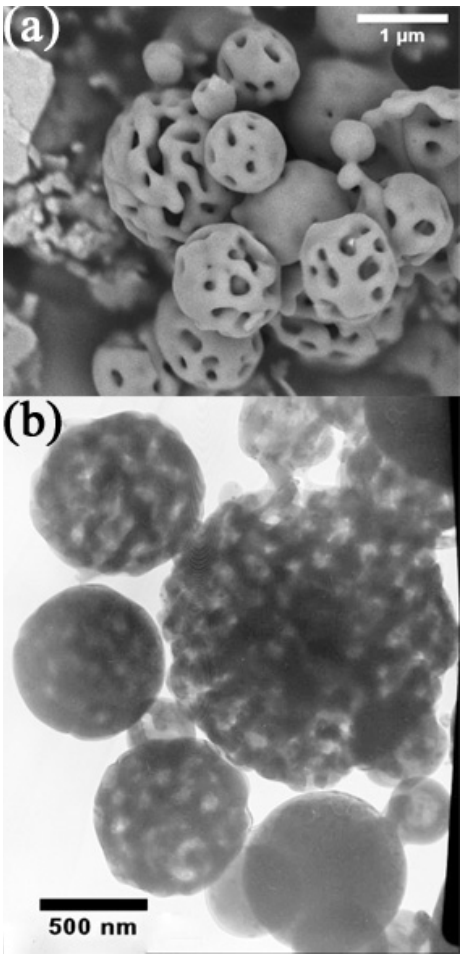

Figure 2. (*a*) SEM and (*b*) TEM imaging of SPG3 powder.

2.3. Experimental set-ups for luminescence characterization

The phosphor powders have been characterized by several means: luminescence excitation spectroscopy (in the UV and VUV ranges) and emission measurements under Hg-lamp or plasma excitation.

The spectroscopy set-up has a SPEX Jobin Yvon (Fluorolog II FL212) spectrofluorimeter. It is coupled with a VTM300 VUV excitation monochromator, equipped with a 200 W D_2 lamp, for the VUV bench. The UV bench is made of a SPEX 1680 double grating monochromator equipped with an XBO W/4 (Suprasil quartz glass) 450 W lamp. The excitation spectrum of sodium salicylate is recorded under the same conditions and is used as a standard to correct the data from the lamp flux and the monochromator response. This

Table 3. Mean values of the absorption coefficients for the SPR and SPG powders in the plasma wavelength domain and at 254 nm.

Absorption coefficient (cm^{-1})	254 nm	Plasma (147 and 173 nm)
SPR	$5 \times 10^4 \pm 50\%$	$10^6 \pm 5\%$
SPG	$10^4 \pm 50\%$	$0.5 \times 10^6 \pm 10\%$

procedure is the one generally applied to correct the excitation spectra because the external quantum efficiency of sodium salicylate is constant in the 40–340 nm excitation range [9, 10]. The corrected excitation spectrum is then determined as follows: raw excitation spectrum/sodium salicylate spectrum. It has been observed that residual short-wavelength light passes through the VUV monochromator operating in the 210–300 nm range, that may be removed by filtering with a quartz plate. For samples CP*i* ($i = R$ or G), excitation spectra have been collected without and with the filter. The correction curves $F_{\mathrm{CP}i} = I_{\mathrm{filtered}}/I_{\mathrm{unfiltered}}$ have then been applied to the observations under unfiltered conditions. With this correction, the spectra observed in the 210–300 nm range with the VUV bench match those obtained with the UV bench. The data of the excitation spectra displayed on figure 3 have been recorded with the VUV device between 120 and 275 nm, and with the UV–visible configuration for the range between 275 and 500 nm. The powders have been deposited in one of the compartments of a rotating holder, and gently pressed with a MgF_2 plate to obtain a smooth surface; the sodium salicylate used as a standard is placed in one of the four compartments. The position of the sample holder and the quality and the position of the sample surface relative to the collimation point of the incident light have non-negligible effects. The reproducibility of the relative intensity measurements is estimated at ±5%. This experimental set-up can be compared with the one already described by Jüstel *et al* [11]. In their work, there was a dry nitrogen flow around the sample. Moreover, they normalized the intensity in the spectra to the absolute value of light efficiency at 254 nm excitation and the results have been validated using synchrotron radiation experiments. The excitation spectra of this work and those displayed in [11] have a similar shape.

On the other hand, in order to work near PDP conditions, we have developed an experimental set-up ('CPAT set-up') to study the emission spectra, relative intensities and transient characteristics of phosphors excited by rare gas discharges. The experimental set-up, as shown in figure 4, consists of a stainless steel chamber filled for this work with Xe at low pressure, typically a few Torr. Under these conditions, the VUV photons are emitted by the resonance states of

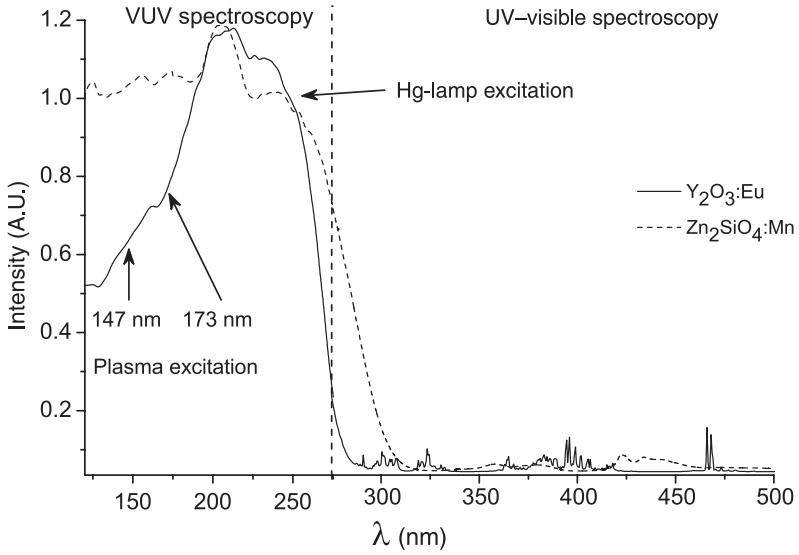

Figure 3. Excitation spectra of the two phosphors in the whole VUV–UV–visible range.

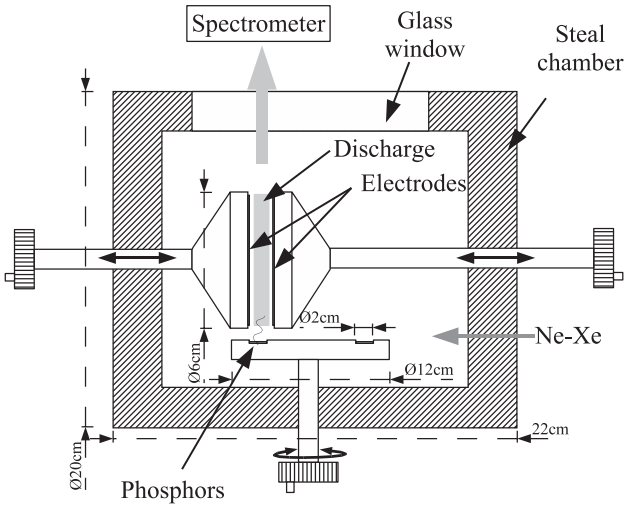

Figure 4. Scheme of the CPAT experimental set-up.

xenon (147 nm) [12]. The discharge is confined between two aluminium electrodes 6 cm in diameter, insulated from the walls by a ceramic. The distance between the electrodes can be tuned between 0.1 and 5.5 cm. Visual observation and spectroscopic measurements are possible through a quartz window at the top of the chamber. A rotating ceramic plate with six compartments can receive five samples and a blank powder ($BaSO_4$) to characterize the plasma and to control the discharge stability. Each compartment is placed successively below the electrodes using a rotary motion. Once the samples are installed, the chamber is evacuated using a standard rotary pump and a turbomolecular pump to 10^{-6} Torr. Then the chamber is filled with xenon (5 Torr). The voltage supply is then connected, and the working conditions are: alternative sinus input voltage, voltage range 100–500 V and frequency range 1–2 MHz. The light emitted by the phosphors and that associated with the gas discharge are collected via an optical fibre through the quartz window, connected to an Avantes SD2000 spectrometer with two gratings (500–780 and 775–1020 nm). The near-IR part of the spectra allows us to characterize the xenon emission [13]. The acquisition time is about 1 s for spectrum measurements. The visible part of the gas discharge emissions is measured on the $BaSO_4$ powder (blank spectrum). Sample emission spectra (displayed in figures 5 and 6) can be obtained by subtracting the blank spectrum from the total spectrum (phosphor sample + discharge). The emission intensity is numerically integrated on the 500–750 nm range of the spectrometer. Measurements to validate the experimental set-up have been done as described in [12]. The reproducibility of the relative intensity measurements is ±6.5%. For the decay analysis, the discharge is modulated at 6 Hz (ON for 30 ms, OFF for 136 ms) and the signal is measured using a photodiode (Centronic OSD15-E) coupled to an operational amplifier and an oscilloscope (Tektronix TDS 714L). The blank time response is also systematically subtracted from the sample's response.

Some of the samples have also been measured with another set-up ('DGTec set-up'), closer to PDP working conditions. In this set-up, the vacuum chamber front glass window supports a grating of co-planar electrodes. After evacuation to 10^{-6} Torr, a gas mixture, Ne–30%Xe, is introduced at 450 Torr. The discharge is ignited and sustained by a 20–50 kHz and 0–1000 V power supply. The rotating sample holder is vertical; it receives three samples and a reference (Al_2O_3). The luminance is measured through the front window using a Photoreasearch Pritchard 1980B spectrophotometer, after filtering by a photopic filter. The integrated intensity is read for each sample successively, and the measure on the reference powder is subtracted. At this gas pressure, the VUV photons are emitted by the resonance (147 nm) and excimer (173 nm) states of xenon [14].

The relative brightness of the samples under 254 nm excitation has also been measured using a 4 W Vilber Lourmat mercury lamp ('Hg-lamp set-up'), the emitted light is measured by reflection on the sample surface using a Photoresearch Pritchard 1980B spectrophotometer, after filtering by a photopic filter. The scattered incident light

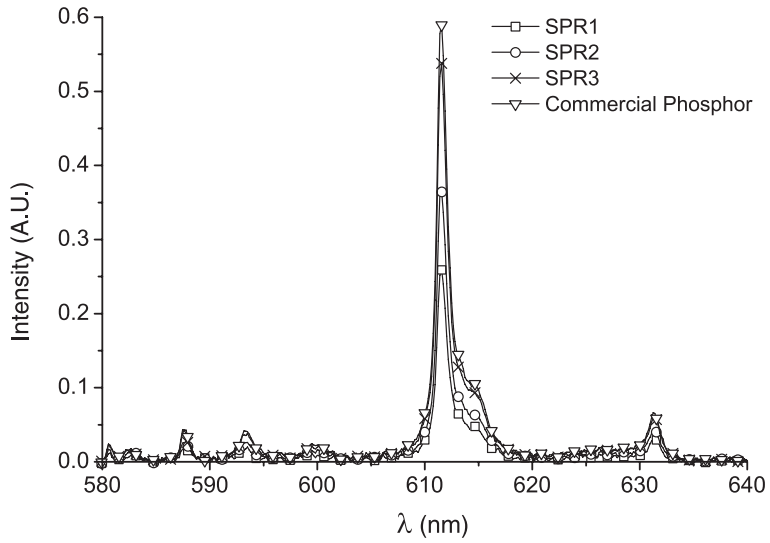

Figure 5. Emission spectra of the SPR series compared with the commercial phosphor one under plasma excitation in the CPAT chamber.

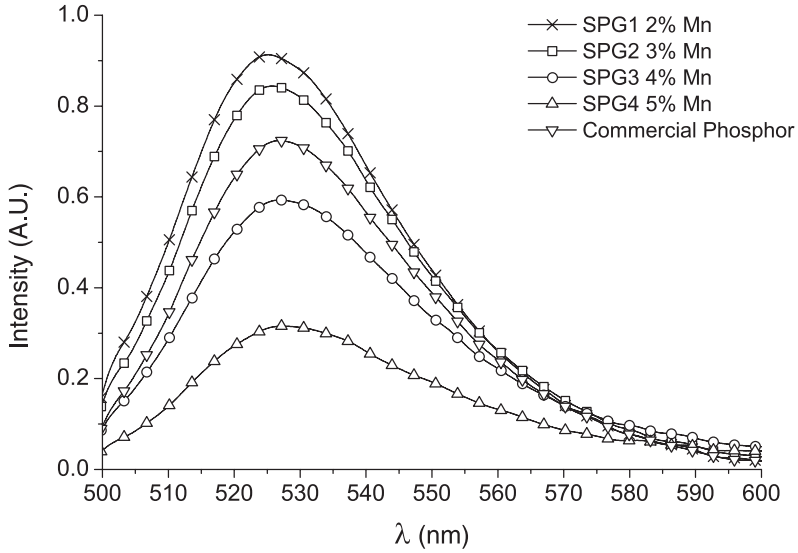

Figure 6. Emission spectra of the SPG series compared with the commercial phosphor one under plasma excitation in the CPAT chamber.

measured under the same conditions on the reference Al_2O_3 is negligible. Results obtained with these set-ups (denoted, respectively, as spectroscopy, Hg lamp, CPAT and DGTec) will be compared in the next sections.

3. Results

3.1. Absorption coefficients

The absorption coefficients measured for the SPR and SPG powders (figure 7) have the same order of magnitude as a function of the wavelength. The curves displayed in the figures correspond to analysis of different grains of the same sample. The values of the absorption coefficient are low near 254 nm compared with those in the plasma domain (147 and 173 nm). They differ by at least one order of magnitude (table 3).

The EELS measurements are not sensitive enough in the high-wavelength domain (over 240 nm) to detect the absorption of the dopant (Eu^{3+} or Mn^{2+}), which should appear as a shoulder on the lattice signal (Y_2O_3 or Zn_2SiO_4, respectively) around 250 nm. In fact, in this wavelength domain, the extraction of the EELS signal cannot be precise. The comparison of EELS results with optical ones (extracted from [15]) in the low-energy domain revealed that the absorption coefficient is higher in the case of EELS. However, this is not the case for the plasma domain, where the two experiments agree well.

3.2. Photoluminescence intensities

The excitation spectra of the SPR, SPG series and commercial red and green (CPR, CPG) phosphors are shown in figures 8 and 9. The dotted line represents the limit between the absorption in the charge transfer state of the dopant ion (higher wavelengths) and that in the host lattice (lower wavelengths): it has been drawn at the minima of the curves, 222 nm for $Y_2O_3:Eu^{3+}$ and 225 nm for $Zn_2SiO_4:Mn^{2+}$. The luminescence efficiencies relative to the commercial

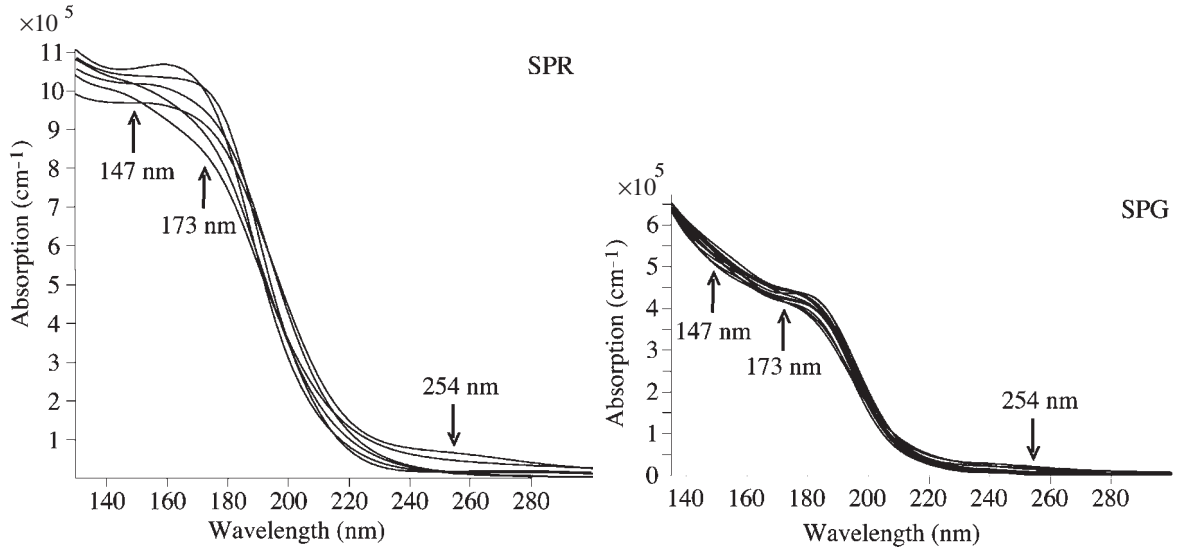

Figure 7. Absorption coefficients extracted from EELS analysis of SPR2 and SPG4 samples.

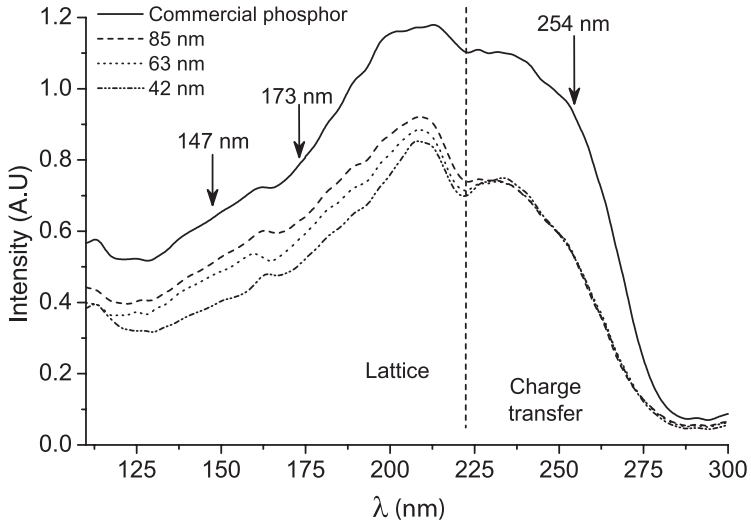

Figure 8. VUV–UV excitation spectra of the red phosphor series.

phosphors have been extracted from these spectra at 254 and 147 nm (tables 1 and 2).

At 254 nm excitation, there is a good agreement of the measurements with the two set-ups 'Hg lamp' and 'spectroscopy'. The efficiencies of the SPR samples (table 1) are the same and are equal to 60% of the CPR, whatever the crystal size. This has been assigned in previous works [4, 5] to (i) the fact that the absorption of the 254 nm radiation is not complete in SPR samples, due to the hollow character of the particles, and (ii) the fact that absorption at 254 nm promotes transitions to the charge transfer state; this electronic state is localized on the europium ions and there is no appreciable diffusion of this energy in the crystals, then there being no effect of the crystal size. The relative efficiencies measured under VUV excitations are quite different from the UV-excited ones. Under plasma excitation (set-ups CPAT and DGTec in table 1), the luminescence efficiencies of the SPR phosphors increase with increasing crystal size (figure 5), SPR3 attaining the CPR one. The energies of the VUV radiations are just above the fundamental absorption edge of the lattice (figure 7). Taking the absorption coefficient $\alpha = 10^6\ \mathrm{cm}^{-1}$ (table 3), one estimates that 90% of the radiation is absorbed over a 25 nm thickness, that is in the particle's outer shell. The VUV energy migrates in the individual crystals before transferring to the europium ions, which explains the observed increase in emitted light with average crystal size. The intensities measured at 147 nm in the excitation spectra (figure 8) also increase from SPR1 to SPR3, but the variation is less steep than observed with the plasma set-ups and the last sample efficiency is only 80% of the CPR. As discussed in the section later, the origins of these discrepancies are till now not fully understood.

The efficiencies of SPG samples at 254 nm excitation amount to 70% of the CPG. There is no appreciable variation with the Mn^{2+} percentage between 2% and 5% Mn/(Mn + Zn) (table 2). The morphology of the SPG particles is not the core–shell one observed in SPR (see figures 1 and 2), but the apparent density in these samples also is low (about $\frac{1}{2}$ of the theoretical one) and the absorption of the 254 nm radiation

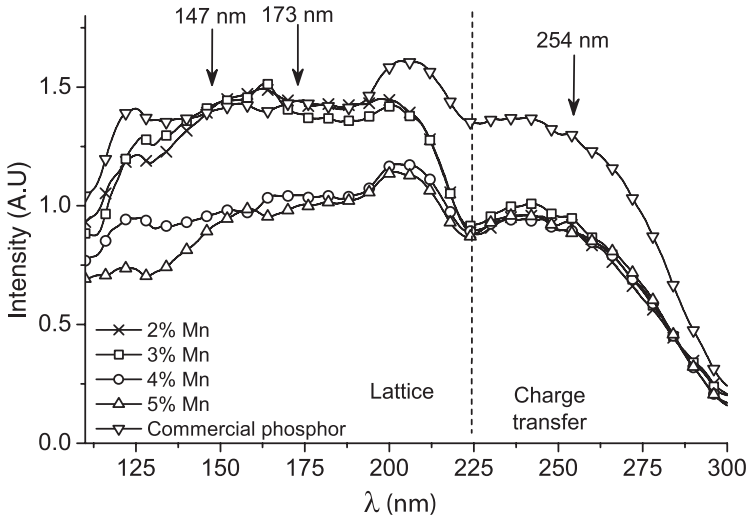

Figure 9. VUV–UV excitation spectra of the green phosphor series.

is not complete. The absorption in the oxygen to manganese charge transfer state increases with the manganese proportion, but at the same time the emitted visible light is more quenched. As a result, we observe that the light efficiency is constant in the composition range investigated. Other authors [16, 17] have observed a maximum efficiency around 5–6% Mn/(Mn + Zn).

The emission of SPG phosphors under VUV excitation decreases steeply with increasing Mn^{2+} content (table 2). This general trend has been observed with all three experimental set-ups, but marked differences remain between the measurements. The excitation spectra (figure 9) for SPG1 and SPG2 (Mn/(Mn + Zn) = 2% and 3%, respectively) almost match, and the same is true for SPG3 and SPG4 (Mn/(Mn + Zn) = 4% and 5%, respectively). At the same time, the emission spectra recorded using the CPAT set-up (figure 6) exhibit a more regular decrease from SPG1 to SPG4. It has been reported in the literature (for instance in [16, 17]) that the efficiency of the manganese-doped willemite green phosphor under VUV excitation decreases between 1% and 10% Mn/(Mn + Zn), which means that the maximum efficiency occurs at still lower contents. So the same trend is observed here; nevertheless, it is really difficult to compare more precisely the observations made by different groups, because the synthesis conditions, i.e. the powders morphologies, have such a strong influence on the efficiencies observed under VUV radiation and on their variation with doping rate as well, specifically for $Zn_2SiO_4 : Mn^{2+}$.

3.3. Photoluminescence decays

The luminescence decays have been analysed using the CPAT set-up, and the 147 nm excitation pulse duration is 30 ms. The three SPR phosphors exhibit the same decay curves; the decay times τ_{10} (measured at 10% of the intensity, I_0, at the end of the pulse) are all equal to 4 ms, within the error range. The CPR decays more slowly, and τ_{10} is 5 ms (table 1).

The τ_{10} values measured for SPG powders decrease rapidly from 36 to 12 ms with Mn content increasing from 2% to 5% (table 2). Van der Kolk *et al* have put forward in [16] the idea that the lifetimes measured under VUV excitation are longer than the ones measured under 254 nm or longer wavelength excitations, indicating that slow relaxation mechanisms affect the Mn luminescence after host lattice excitation. Also, excitation pulses longer than 5 ms induce an increase in the apparent decay times. The value given for 2.5% Mn/(Mn + Zn), $\tau_{10} = 17$ ms, has been measured under a microsecond pulse and it is reported that for a 5 ms pulse the apparent τ_{10} is 5 ms longer. It turns out to be 22 ms, whereas our values are 36 ms and 29 ms for Mn/(Mn + Zn) = 2% and 3%, respectively. Regarding the samples prepared by spray pyrolysis, the value $\tau_{10} = 7$ ms at 5% Mn/(Mn + Zn) has been reported by Kang and Park [18], but the details of experimentation are not given, whereas we measure 12 ms. There is a spreading of the numerical values reported. Besides the uncertainties in the determinations (generally ±10%), important effects are caused by the mechanisms of energy transfer in the host towards the emitting ions, which makes the proper description of the experimental conditions crucial. It may be underlined that CPG and SPG3 phosphors, both with 4% Mn/(Mn + Zn), exhibit quite similar decay functions when recorded under the same conditions (table 3), which is a proof that the mechanisms involved are directly connected to the phosphor composition, and much less influenced by the morphology than the intensity variation.

4. Discussion

All measurements performed in the UV excitation range with the excitation spectroscopy set-up on the one hand and with Hg-lamp excitation on the other hand are in very good agreement for both series of phosphors. The relative efficiencies measured for excitation in the VUV range agree much less. The possible artefacts originating from the different devices have been considered and as far as possible corrected. One problem of major importance nevertheless remains: the sample preparation for the measurements. It appears that points like the macroscopic surface roughness, or the exact position of the sample with respect to the incident radiation and to the optical set-up, are of major importance when considering high-energy incident radiations. In contrast, the VUV-excited

emission decay curves do not suffer from possible non-reproducibility in the sample preparation. The decays are not exponential, and will be characterized, as usual, by τ_{10}, which is appropriate for comparing data measured under similar experimental conditions.

All the observations made highlighted the differences between the phosphor responses at 254 nm excitation and at higher energy excitations. At 254 nm excitation, the SPR and SPG phosphors never reach the luminescence efficiencies of the commercial phosphors, CPR and CPG. At VUV excitation, the red phosphor $Y_2O_3:Eu^{3+}$ prepared by spray pyrolysis and submitted to proper annealing (SPR3) attains the luminescence characteristics of CPR. But the luminescence characteristics of CPG (100% efficiency and $\tau_{10} = 17.5$ ms) were not attained simultaneously by one of the SPG samples. The efficiency of SPG1 ($Mn/(Mn + Zn) = 2\%$) is $130\% \pm 10\%$ that of the commercial phosphor (CPG, $Mn/(Mn + Zn) = 4\%$), and the decay time τ_{10} is equal to 36 ms. On the other hand, the same decay time as for CPG, $\tau_{10} = 17.5$ ms, is observed with SPG3 (4% Mn/(Mn+Zn)), but the measured efficiency is only $80\% \pm 10\%$. It must be mentioned that another group (Kang and Park [18]) claims to have succeeded in obtaining the proper characteristics of spray pyrolysed green phosphors.

Because the natures of the transitions responsible for the absorptions of the two radiations are quite different, the penetration depths of the incident radiations also differ by at least one order of magnitude: 90% of the 254 nm incident radiation is absorbed over 500–2500 nm with the coefficients in table 3, whereas 90% of the VUV radiation is absorbed over 25–50 nm. Bechtel *et al* [19] have also underlined the fact that the limited size of the volume excited in the phosphor must be taken into account in PDP applications. They estimate the penetration depth of VUV excitation at 100–200 nm. It has been shown in [5] that the core–shell morphology of the spherical particles in spray pyrolysed red phosphors (SPRs) allows us to understand why these powders exhibit a relatively low efficiency at 254 nm excitation, while they attain the CPR efficiency at VUV excitations. The morphology of spray pyrolysed green phosphors (SPGs), with a lot of open porosity at the surface of the spheres, is very probably the cause of the failure to observe 100% efficiency relative to the commercial green phosphor (CPG) of the same composition, even with VUV excitation. The fact that the same decay curves have been recorded for SPG3 and CPG suggests that the luminescence build-up, the concentration quenching and even the quenching at structural or chemical defects are the same in the two samples and are not modified by the surface morphology. Thus we conclude that the porous morphology alters the absorption, and maybe the light scattering of the green phosphors.

5. Conclusion

We have used the technique of spray pyrolysis to prepare red and green phosphors ($Y_2O_3:Eu^{3+}$ and $Zn_2SiO_4:Mn^{2+}$, respectively) for PDPs. Different techniques have been employed for investigation of the optical properties of the prepared powders, especially in the VUV energy range. Characteristics of the red and green phosphors from spray pyrolysis (SPR and SPG) have been compared with those of the corresponding commercial phosphors (CPR and CPG). Some discrepancies still remain between the observations made with the different set-ups, highlighting the difficulty in quantifying properly the emission efficiencies. The red phosphors prepared by spray pyrolysis and submitted to appropriate annealing attain the luminescence characteristics of the commercial phosphor under plasma excitation and can be proposed for PDP applications, but the characteristics of the commercial green phosphor, its efficiency and decay time, have not been attained simultaneously.

Acknowledgments

This work was supported by the Ministère de la Recherche (RNMP/POSUMIC). The authors wish to thank RHODIA for supplying the lanthanide solution and Thomson Plasma for the measurements under plasma excitation. The SEM images have been taken at the Service de Microscopie Electronique (UPS, Toulouse).

References

[1] Gurav A, Kodas T, Pluym T and Xiong Y 1993 *Aerosol Sci. Technol.* **19** 411–52
[2] Joffin N 2004 Synthèse par pyrolyse d'aérosol et caractérisation de luminophores: $Y_2O_3:Eu^{3+}$ et $Zn_2SiO_4:Mn^{2+}$ pour applications dans les panneaux à plasma *Thèse* Institut National Polytechnique Toulouse, France
[3] Alavi S, Caussat B, Couderc J P, Dexpert-Ghys J, Joffin N, Neumeyer D and Verelst M 2002 *Advances in Science and Technology* vol 30A, ed P Vincenzini (Faenza: Techna) pp 417–24
[4] Joffin N, Baret G, Dexpert-Ghys J, Verelst M, Baules P and Garcia A 2003 *VDI-Berichte* vol 1803 (Nanofair 2003: New Ideas for Industry) pp 231–5
[5] Joffin N, Dexpert-Ghys J, Verelst M, Baret G and Garcia A 2005 *J. Lumin.* at press
[6] Schamm S and Zanchi G 2001 *Ultramicroscopy* **88** 211
[7] Moine B, Mugnier J, Boyer D, Mahiou R, Schamm S and Zanchi G 2001 *J. Alloys Compounds* **816** 323–4
[8] Egerton R F 1996 *Electron Energy-Loss Spectroscopy in the Electron Microscope* 2nd edn (New York: Plenum)
[9] Mayolet A 1975 Etude des processus d'absorption et de transfert d'énergie au sein de matériaux inorganiques luminescents dans le domaine de l'UV et VUV *Thèse* Université Paris-XI, Orsay, France
[10] Samson J A R 1977 *Techniques of Vacuum Ultraviolet Spectroscopy* vol 212 (New York: Wiley)
[11] Jüstel T, Krupa J C and Wiechert D U 2001 *J. Lumin.* **93** 179–89
[12] Caillier B, Guillot Ph, Galy J, Mauricot R, Dexpert-Ghys J and Joffin N 2004 *15th International Conf. on Gas Discharges and their Applications* (*Toulouse*)
[13] Ouyang J T, Callegari Th, Caillier B and Boeuf J P 2003 *J. Phys. D: Appl. Phys.* **36** 1959–66
[14] Audray G, Guillot Ph, Galy J and Brunet H 1999 *Euro Display 99 (Berlin, Germany)*
[15] Palik E D ed 1991 *Handbook of Optical Constants of Solids* 2nd edn (Boston, MA: Academic)
[16] Van der Kolk E, Dorenbos P, Van Eijk C W E, Bechtel H, Justel T, Nikol H, Ronda C R and Wiechert D U 2000 *J. Lumin.* **87** 1246
[17] Sohn K S, Cho B and Park H D 1999 *Mater. Lett.* **41** 303
[18] Kang Y C and Park H D 2003 *Appl. Phys.* A **77** 529
[19] Bechtel H, Jüstel T, Gläster H and Wiechert D U 2000 *SID 2000* p 366